Environ. Sci. Technol. **2005**, *39,* 577−584

Hydrodynamic Aspects of Particle Clogging in Porous Media

DAVID C. MAYS* AND JAMES R. HUNT
Department of Civil and Environmental Engineering, University of California at Berkeley, Berkeley, California 94720-1710

Data from 6 filtration studies, representing 43 experiments, are analyzed with a simplified version of the single-parameter O'Melia and Ali clogging model. The model parameter displays a systematic dependence on fluid velocity, which was an independent variable in each study. A cake filtration model also explains the data from one filtration study by varying a single, velocity-dependent parameter, highlighting that clogging models, because they are empirical, are not unique. Limited experimental data indicate exponential depth dependence of particle accumulation, whose impact on clogging is quantified with an extended O'Melia and Ali model. The resulting two-parameter model successfully describes the increased clogging that is always observed in the top segment of a filter. However, even after accounting for particle penetration, the two-parameter model suggests that a velocity-dependent parameter representing deposit morphology must also be included to explain the data. Most of the experimental data are described by the single-parameter O'Melia and Ali model, and the model parameter is correlated to the collector Peclet number.

Introduction

Permeability reduction caused by particle deposition in porous media, or *clogging*, is important in several contexts. The operation of deep-bed filters for water treatment is constrained by the available head loss (*1*). In natural aquifers, controlling permeability is essential for the operation of injection or extraction wells and in quantifying contaminant mobility (*2*−*4*). Clogging is relevant to enhanced bioremediation, since microbial growth alters flow and transport (*5*). Stream interaction with bed sediments is largely determined by particle accumulation in the streambed sediments (*6*). In addition, erosion of colloidal deposits has been proposed as a key mechanism to explain the rapid response of aquifers and streamflows to distant earthquakes (*7*).

Both solution chemistry and hydrodynamics are known to alter the permeability of porous media containing colloidal particles. Solution pH, ionic strength, and exchangeable ions determine colloid stability and hence the morphology of deposited colloids and the resulting permeability of the formation (e.g., refs *8* and *9*). In contrast, there have been fewer studies on the effect of hydrodynamics. Importantly, several studies have noted that, for a given mass of deposited material, experiments conducted at greater fluid velocity show greater permeability (*10*−*12*). There is also recognition in a few studies that sudden changes in fluid velocity can alter the permeability of filters containing retained particles (e.g., refs *13* and *14*).

* Corresponding author phone: (510) 486-7083; fax: (510) 486-5686; e-mail: mays@ce.berkeley.edu.

Available models for clogging based on first principles are not predictive due to the structural complexity of colloidal deposits and the difficulty in quantifying feedback between the flow and the deposit. Tien (*1*) reviewed clogging models based on the Kozeny−Carman equation, noting that all require empirical parameters. Tien (*1*) also noted that clogging models based on growth of particle dendrites from collector surfaces have not been successful at predicting permeability, and Wiesner (*15*) cautioned that such models are computationally intractable. Recent models based on random networks of constricted tubes predict permeability reduction with particle accumulation but are based on geometric simplifications and include no data for comparison (e.g., refs *16* and *17*).

Given the broad relevance of clogging and the lack of predictive models, this work analyzes published data on clogging from carefully controlled laboratory experiments. The goal is to couple flow hydrodynamics with permeability reduction during clogging through an empirical representation of deposit morphology.

Overview of Clogging Data

Eight sources of clogging data are described in Table 1 (*11*, *18*−*24*). Each study reports clogging resulting from favorable deposition in saturated porous media. These studies were selected because they varied the fluid velocity as an independent variable, except for Tobiason and Vigneswaran (*21*), as discussed below. As shown in Table 1, four of these data sets include clogging data within the filter as a function of depth, x, which will be used in Model for Depth-Dependent Data to analyze the depth of particle penetration.

Under constant-flow conditions, clogging is observed through a head loss, ΔH, that exceeds the clean bed head loss, ΔH_o. Permeability reduction is reported as normalized increase in head loss, $\Delta H/\Delta H_o - 1$, which allows clearer data visualization and comparison with theory. When influent and effluent particle concentrations are known over time, the quantity of deposited particles is determined by mass balance. The specific deposit, σ, is calculated by dividing the deposited mass by the particle density and the total filter volume.

Inspection of clogging data reveals four observations that will be the basis for two different modeling approaches. These observations are illustrated for 24 experiments from Veerapaneni (*23*) in Figure 1. Data from other sources are presented in Figures S1−S7 of the Supporting Information.

(1) For a given specific deposit, experiments conducted with smaller fluid velocity have larger head loss. This hydrodynamic effect is clearly visible in four data sets (see Figures 1, S1−S3). In four others, where the ratio of maximum to minimum fluid velocity is less than 3.5, this effect is not apparent (see Figures S4−S7).

(2) The specific deposit for each experiment represents less than 1% of the filter volume, even when the head loss increases by 2−3 orders of magnitude (see Figures 1 and S6). With media porosity near 40%, this suggests that clogging does not depend primarily on porosity reduction.

(3) When clogging is slight, taken as $\Delta H/\Delta H_o - 1 < 10$, the normalized increase in head loss scales linearly with specific deposit, indicated by a 1:1 slope when plotted on log−log axes. This is observed in all but two of the six data sets with slight clogging (see Figures S2, S3, S5, and S7).

(4) When clogging is severe, taken as $\Delta H/\Delta H_o - 1 > 10$, the normalized increase in head loss scales quadratically with specific deposit, indicated by a 2:1 slope (see Figures 1 and S6).

10.1021/es049367k CCC: $30.25
Published on Web 12/09/2004

TABLE 1. Technical Details on Filtration Experiments and Power Law Exponents for Model Parameters that Depend on Fluid Velocity. Angled Brackets Indicate Estimated Values

first author	Narayan	Perera	Chang	Vigneswaran	Tobiason	Boller	Veerapaneni	Al-Abduwani
reference	(*11*)	(*18*)	(*19*)	(*20*)	(*21*)	(*22*)	(*23*)	(*24*)
raw data in Figure	S3	S1	S2	S4	S5	S6	1	S7
no. of experiments	5	4	4	11	4	3	24	3
ΔH data at multiple depths	no	yes	yes	no	no	no	yes	yes
σ data at multiple depths	no	yes	yes	no	no	no	no	yes
slowest velocity (cm/s)	0.030	0.14	0.13	0.14	0.14	0.19	0.0067	0.27
fastest velocity (cm/s)	0.30	0.56	0.39	0.47	0.14	0.62	0.51	0.55
velocity ratio	10	4.0	3.0	3.4	1	3.3	76	2.0
clogging depends on velocity?	yes	yes	yes	no	no	no	yes	no
fluid	kerosene	water	water	water	water	water	water	water
destabilization	none	alum	polymer	<polymer>	Ca^{2+} polymer	<alum or polymer>	Ca^{2+}	electrostatic
particle	carbon black	kaolinite	kaolinite	kaolinite	polystyrene	iron hydroxide	latex	hematite
particle diameter (μm)	8	⟨1⟩	⟨1⟩	⟨1⟩	0.27 1.3 10	⟨0.1⟩	0.044 0.069 0.090	⟨0.085⟩
particle density (g/cm^3)	1.8	⟨2.7⟩	⟨2.7⟩	⟨2.7⟩	⟨1.05⟩	⟨2.5⟩	1.05	⟨5.3⟩
influent concentration (mg/l)	96−200	100	100	80	10		3−26	20−78
filter length (cm)	30	32.5	40	2	17	5−15	2	12.7
collector	glass	sand	sand	glass	glass	sand	glass	sandstone
mean collector diameter (μm)	930	710	1200	350	400	1400	360	120
porosity	0.37	0.46	0.44	⟨0.4⟩	⟨0.4⟩	0.4	0.4	0.22
filter averaged $\gamma \sim u^n$	−0.56		−0.94				−0.85	
depth dependent $\delta \sim u^n$			0.72				0.77	
depth dependent $\gamma_2 \sim u^n$			−0.79				−0.69	

These four observations will guide the development of the clogging models in Models for Filter-Averaged Data.

Wright (*25*) studied deposition of kaolinite clay in two sand filters at various flow rates. In subsequent analysis of these data, evaluated over segments of the filter shorter than 5.7 cm, Hunt et al. (*26*) observed the normalized increase in head loss scaled as $\sigma^{2/3}$, shown in Figures 4 and 5 of Hunt et al. (*26*), contradicting the observations discussed above. This lack of agreement may result from the fact that Wright's experimental apparatus included sampling ports that intermittently withdrew fluid and colloids along the length of the column. As Wright (*25*) stated, this may have disturbed the deposits and contributed to additional uncertainty in the concentration measurements. For this reason, further analysis of these data was not attempted.

Models for Filter-Averaged Data

Two models are considered to describe clogging, first as a deep-bed filtration process and then as a cake filtration process. Both models start with Darcy's law

$$u = -\frac{k\rho g}{\mu}\frac{\Delta H}{\Delta x} \tag{1}$$

where u is the approach velocity, k is the permeability, ρ is the fluid density, g is the acceleration of gravity, μ is the fluid dynamic viscosity, and x is measured in the direction of fluid flow.

Deep-Bed Filtration Model. (1) Model Derivation. O'Melia and Ali (*27*) began with the observation that permeability depends inversely on the square of the surface area within the filter (*28*):

$$k \propto M^{-2} \tag{2}$$

where M is specific area or surface area per bed volume. The ratio of head loss to clean bed head loss is

$$\frac{\Delta H}{\Delta H_o} = \frac{k_o}{k} = \left(\frac{M}{M_o}\right)^2 \tag{3}$$

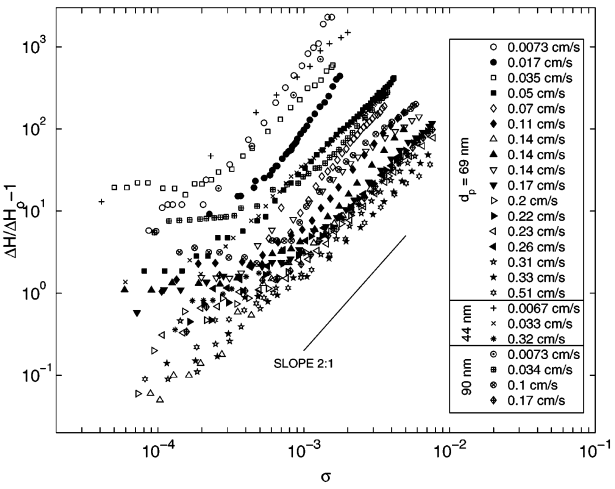

FIGURE 1. Normalized increase in head loss versus specific deposit from Veerapaneni (*23*).

where k_o is the clean bed permeability and M_o is clean bed specific area. For a clean filter with porosity ϵ composed of spherical collectors of diameter d_c, the clean bed specific area is

$$M_o = 6(1-\epsilon)/d_c \tag{4}$$

As particles accumulate on the collector, its surface area increases proportional to the number of deposited particles,

$$A_c = \pi d_c^{\,2} + \beta' N A_p^{\,2} \tag{5}$$

where A_c is the surface area per collector, β' is an empirical coefficient representing the fraction of retained particles contributing to the increased specific area, N is the number of particles per collector, and A_p is the surface area per particle. The notation β' is used for consistency with previous literature

(e.g., refs *1*, *20*, and *27*). The bed volume per collector, which is constant, is given by

$$V_c = (\pi/6)d_c^3/(1-\epsilon) \quad (6)$$

Combining (5) and (6) gives the specific area for the clogging filter,

$$M = 6(1-\epsilon)\left(\frac{1}{d_c} + \frac{\beta' N A_p}{\pi d_c^3}\right) \quad (7)$$

Equation 7 corrects O'Melia and Ali (*27*), whose derivation assumed that bed volume increases with deposition. Substituting (4) and (7) into (3) gives

$$\frac{\Delta H}{\Delta H_o} = \left[1 + \frac{\beta' N A_p}{\pi d_c^2}\right]^2 \quad (8)$$

There is a one-to-one correspondence between number of particles attached and the specific deposit, σ through

$$N = \frac{\pi d_c^3}{6(1-\epsilon)V_p}\sigma \quad (9)$$

where V_p is the volume per particle. Substituting (9) into (8) gives

$$\Delta H/\Delta H_o = [1 + \gamma\sigma]^2 \quad (10)$$

where

$$\gamma = \frac{\beta' d_c}{6(1-\epsilon)}\frac{A_p}{V_p} \quad (11)$$

Equation 10 is a simple relationship between head loss and specific deposit that uses a single parameter, γ, which includes the particle surface area-to-volume ratio, A_p/V_p, and the empirical parameter, β'. These equations are formally equivalent to eq 14 in Tobiason and Vigneswaran (*21*), which was derived in a different way. Equation 10 can be rewritten as the normalized increase in head loss

$$\Delta H/\Delta H_o - 1 = 2\gamma\sigma + (\gamma\sigma)^2 \quad (12)$$

which indicates a transition from linear to quadratic dependence on specific deposit. This aspect of the O'Melia and Ali model was previously noted by Darby et al. (*29*).

For each experiment in the eight data sets, the parameter γ was chosen to minimize the sum of the squared residuals, with residuals defined as the difference between $\ln(\Delta H/\Delta H_o - 1)$ and $\ln[2\gamma\sigma + (\gamma\sigma)^2]$. The logarithmic transform was used to avoid overweighting the few largest data. Error bars for γ were estimated using a Monte Carlo procedure as follows. The nominal uncertainty in head loss was assumed to be the larger of ±0.1 cm or ±1% of the maximum head loss, except for Al-Abduwani et al. (*24*), for which the nominal uncertainty was calculated from the clean bed permeability and the reported error in flow rate. Head loss measurements were assumed to be normally distributed about observed values, with standard deviation equal to half the nominal uncertainty. For each of 1000 Monte Carlo steps, head data were replaced with randomly selected substitutes. Then the parameter γ was fitted to the substitute data. When ΔH_o was estimated from the clean bed permeability, rather than assuming it to be the first ΔH datum, it was considered fixed. Specific deposit was also considered fixed, ignoring uncertainty in concentration measurements. It should be emphasized that this procedure does not indicate how well the model fits the data

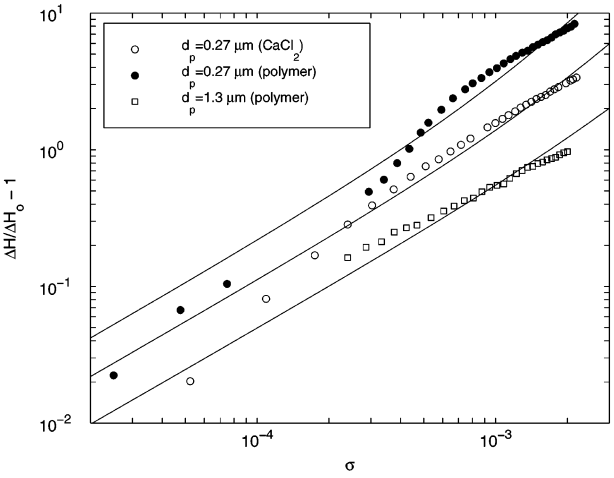

FIGURE 2. Fitted O'Melia and Ali clogging model for three experiments from Tobiason and Vigneswaran (*21*). All experiments have the same velocity $u = 0.14$ cm/s but differ in particle size or coagulant (in parentheses).

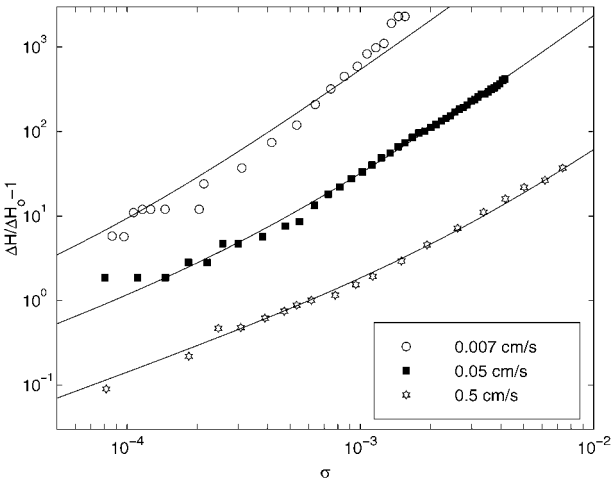

FIGURE 3. Fitted O'Melia and Ali clogging model for three experiments from Veerapaneni (*23*) where $d_p = 0.069$ μm.

but instead estimates the uncertainty in γ resulting from uncertainty in the head loss measurements. Estimated errors were larger than plotted symbols only for Narayan et al. (*11*) and Al-Abduwani et al. (*24*).

(2) Application to Clogging Data. Adjusting the single parameter in eq 10 is sufficient to describe six of the eight data sets. When clogging is slight, the model captures the linear scaling of normalized increase in head loss on specific deposit, illustrated for the data of Tobiason and Vigneswaran (*21*) in Figure 2. This correspondence is also notable because it demonstrates that the O'Melia and Ali clogging model provides a reasonable description of this data set, contrary to the finding in Tobiason and Vigneswaran (*21*). Fitted models for Chang (*19*), Narayan et al. (*11*), and Al-Abduwani et al. (*24*) also capture the observed linear scaling with specific deposit, as illustrated in Supporting Information, Figures S8−S10, respectively. For the two data sets with severe clogging, the model captures the transition from linear to quadratic scaling with specific deposit: Veerapaneni (*23*) is shown in Figure 3; Boller and Kavanaugh (*22*) is shown in Supporting Information, Figure S11. Fitted γ values for these six data sets are given in Supporting Information, Table S1. The model provides a poor description of the two data sets with slight clogging that did not show linear scaling with specific deposit: Perera (*18*) and Vigneswaran and Chang (*20*), shown in Supporting Information, Figures S12 and S13, respectively.

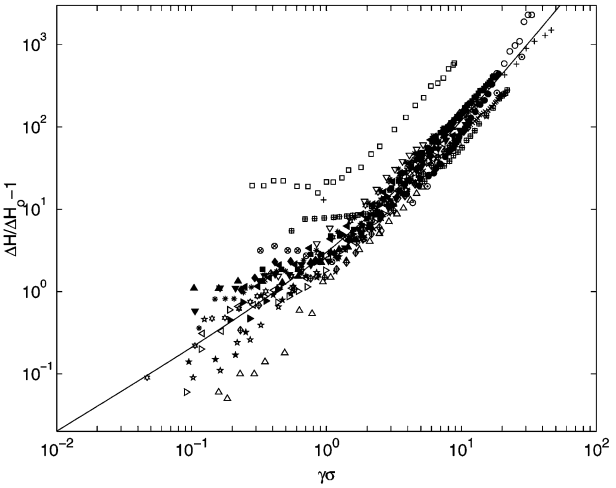

FIGURE 4. Data from Veerapaneni (*23*), rescaled to eliminate the velocity dependence in Figure 1. The abscissa is rescaled by γ, predicted from velocity using empirical eq 13. Symbols are given in Figure 1.

The hydrodynamic effect on clogging is quantified as a power law relationship between the parameter γ and the velocity. For example, the power law relationship for Veerapaneni (*23*) is

$$\gamma = 330u^{-0.85} \tag{13}$$

Since the O'Melia and Ali parameter β' is linearly related to the parameter γ, the observed power law scaling is similar to that reported in Tien (*1*) and Chang (*19*), $\beta' \sim u^{-0.53}$ and $\beta' \sim u^{-0.69}$ for data from Perera (*18*) and Chang (*19*), respectively. This empirical relationship between the parameter γ and velocity suggests a normalization that accounts for the hydrodynamic effect on clogging. Figure 4 shows normalized increase in head loss plotted versus $\gamma\sigma$, with γ predicted from velocity by eq 13. Plotting the data in this manner eliminates the velocity dependence seen in Figure 1. Physically, $\gamma\sigma$ is the ratio of effective deposit surface area to collector surface area within the porous medium, with the effective deposit area defined as the total area of deposited particles multiplied by the empirical factor β'. For $\gamma\sigma \ll 1$, most of the drag is imposed by the collectors with a sparse coating of deposited particles, so eq 12 indicates that $\Delta H/\Delta H_o - 1 \sim \sigma$. For $\gamma\sigma \gg 1$, most of the drag is imposed by flow through the deposited particles, so $\Delta H/\Delta H_o - 1 \sim \sigma^2$. Similarly, normalized data for Chang (*19*) and Narayan et al. (*11*) are shown in Supporting Information, Figures S14 and S15, respectively.

Cake Filtration Model. Models for cake filtration are usually applied to membrane separation systems, where the particles accumulate above the membrane. Head loss occurs separately across the membrane itself, whose permeability is constant, and the filter cake, where head loss increases as the deposit grows or compresses. The permeability and porosity of the filter cake are described with empirical constitutive equations that depend on the compressive stress in the solid phase, the pressure in the fluid phase, and the distance from the membrane. Cake models may be applied to deposition within porous media if one conceptualizes the clean bed as the support matrix on which the particles deposit. Tiab and Donaldson (*30*) employed such a conceptual model to describe permeability reduction resulting from particle injection into a petroleum reservoir.

The cake filtration model is simplified from that presented in Lee and Wang (*31*) by assuming a homogeneous deposit with constant porosity. Total head loss is summed across the clean bed, ΔH_o, and across the cake, ΔH_c

$$\Delta H = \Delta H_o + \Delta H_c \tag{14}$$

Accordingly, the normalized increase in head loss, $\Delta H/\Delta H_o - 1$, is given by $\Delta H_c/\Delta H_o$. Effective cake thickness, L_c, is related to the average specific deposit through

$$L_c = \frac{L}{(1-\epsilon_c)}\sigma \tag{15}$$

where L is the filter length and ϵ_c is the cake porosity. Since σ is increasing, eq 15 models deposit growth. The cake model assumes a constitutive equation for cake permeability that depends on the head loss across the cake, ΔH_c, and an empirical factor, Θ, that represents a threshold compressive stress above which the cake deforms (*31*):

$$k_c = k_{c,o}(1 + \Delta H_c/\Theta)^{-1/2} \tag{16}$$

where k_c is cake permeability and $k_{c,o}$ is cake permeability when the head loss across the cake is zero. An implicit equation for head loss across the filter cake is obtained by substituting (15) and (16) into Darcy's law resulting in

$$\Delta H_c = \frac{u\mu L\sigma}{\rho g k_{c,o}(1-\epsilon_c)}\left(1 + \frac{\Delta H_c}{\Theta}\right)^{1/2} \tag{17}$$

Solving this quadratic equation for $\Delta H_c/\Delta H_o$ gives

$$\frac{\Delta H_c}{\Delta H_o} = \frac{\Delta H}{\Delta H_o} - 1 = \frac{1}{2\Delta H_o}\left[\frac{b^2u^2\sigma^2}{\Theta} + \left(\frac{b^4u^4\sigma^4}{\Theta^2} + 4b^2u^2\sigma^2\right)^{1/2}\right] \tag{18}$$

where

$$b = \mu L/\rho g k_{c,o}(1-\epsilon_c) \tag{19}$$

Equation 18 predicts head loss as a function of specific deposit using two parameters: Θ, representing the compressive strength of the deposit, and the term $k_{c,o}(1-\epsilon_c)$, characterizing the deposit under no-flow conditions. The two terms within the square root expression in eq 18 are equal when

$$\sigma = \sigma^* = 2\Theta/bu \tag{20}$$

The normalized increase in head loss increases linearly with specific deposit when $\sigma \ll \sigma^*$ and quadratically when $\sigma \gg \sigma^*$.

The cake model can be fitted to the 24 experiments of Veerapaneni (*23*) by varying Θ and assuming a constant value of $k_{c,o}(1-\epsilon_c) = 5 \times 10^{-10}$ cm^2, corresponding to the reasonable values of $k_{c,o} = 5$ darcy and $\epsilon_c = 99\%$. Example fits are shown in Supporting Information, Figure S16, and fitted parameters are tabulated in Supporting Information Table S1. There is a consistent velocity dependence of Θ, as shown in Figure S17, with a power law relationship $\Theta = 700u^{2.7}$. When this power law relationship is used to normalize specific deposit and head loss data, the velocity dependence is eliminated (Figure S18). The ability of an empirical cake filtration model to represent the same data modeled by the O'Melia and Ali representation shows that such models are not unique.

Model for Depth-Dependent Data

To recapitulate, inspection of clogging data reveals that permeability depends on fluid velocity (Overview of Clogging Data), and clogging models allow quantification of this effect through an empirical relationship between the parameter γ or Θ and fluid velocity (Models for Filter-Averaged Data). There are at least two possible explanations for the observed

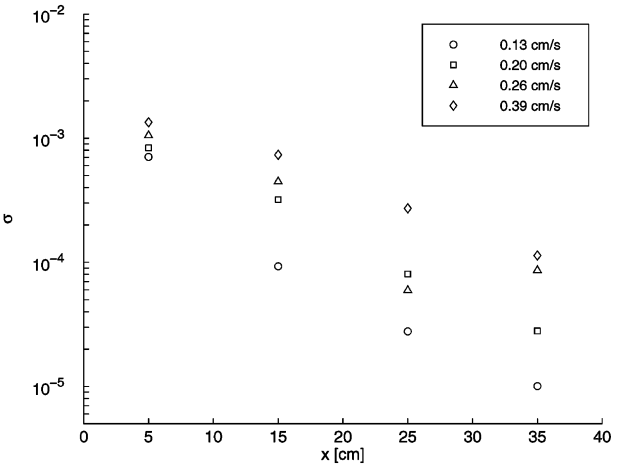

FIGURE 5. Specific deposit versus filter depth for Chang (*19*), indicating the deposit distribution $\sigma(x)$ is approximately exponential. Data calculated over the first 30 min of filtration.

dependence of clogging on velocity: Kau and Lawler (*10*) proposed that fluid velocity controls the depth of particle penetration, while Veerapaneni and Wiesner (*12*, *15*, *32*) proposed that fluid velocity controls deposit morphology. Parameters from the filter-averaged models, γ or Θ, implicitly include both of these effects. The depth of particle penetration is important because clogging is not linear with specific deposit. Other things being equal, a filter with specific deposit 2σ in the top half and zero in the bottom half will be less permeable than a filter with specific deposit σ throughout, which was the assumed deposit configuration in the filter-averaged models presented above. To model particle penetration quantitatively, data taken at intermediate points along the filter will be analyzed to suggest a simple functional relationship for the deposit distribution, $\sigma(x)$, which will then be incorporated in the algebraically simpler O'Melia and Ali clogging model.

Deposit Distribution in Clogging Filters. Perera (*18*), Chang (*19*), and Al-Abduwani et al. (*24*) measured permeability and specific deposit in the top section of their filters. Additionally, Veerapaneni (*23*) measured head loss at an intermediate point within his 2-cm column. All the available data indicate nonuniform particle distribution, even for very short filter lengths.

To highlight the problem resulting from assuming uniform deposit distribution, the O'Melia and Ali parameter γ is fitted to data from Chang (*19*) collected over various filter lengths. These results indicate that the fitted γ increases with column length, corresponding to increasingly unrealistic assumptions of uniform particle distribution (Supporting Information, Figure S19). This dependence of γ on column length motivates the need for an improved clogging model that accounts for the distribution of deposited particles.

Data available in Chang (*19*) and Al-Abduwani et al. (*24*) indicate that the deposit distribution, $\sigma(x)$, is approximately exponential for clogging filters, shown in Figure 5 and Supporting Information, Figure S20. Such analysis was not possible for Perera (*18*), who reported data over only two intervals. Filtration theory predicts an exponential distribution of particles only in the initial phase of deposition (*2*), but an exponential deposit is certainly more realistic than a uniform deposit.

Extension of O'Melia and Ali Model. The goal in this section is to extend the O'Melia and Ali model to utilize filter-averaged head loss and mass balance data, intermediate head loss data, and the assumption of exponential deposit distribution to simultaneously estimate a characteristic depth of particle penetration, δ, and a redefined morphology parameter, γ_2. The approach is similar to that presented by Bedrikovetsky et al. (*33*), who also used intermediate head loss to estimate the deposit distribution, but used an additional assumption about filtration efficiency as a substitute for specific deposit data.

The specific deposit is assumed to decay exponentially with depth

$$\sigma(x,t) = \sigma_o(t)e^{-x/\delta} \tag{21}$$

where δ is the characteristic depth of particle penetration and $\sigma_o(t)$ is the value of the specific deposit at the surface of the filter at time t. The surface value of the specific deposit can be estimated from the segment-averaged specific deposit at time t, $\sigma(t)$ through

$$\sigma_o(t) = \frac{L\sigma(t)}{\delta(1 - e^{-L/\delta})} \tag{22}$$

The O'Melia and Ali model is assumed to be locally valid,

$$\frac{dH}{dx} = \frac{dH_o}{dx}[1 + \gamma_2\sigma(x)]^2 \tag{23}$$

where γ_2 is the morphology parameter appropriate for this two-parameter model. Utilizing a differential form of Darcy's law, eq 23 can be integrated using the boundary condition of $H = 0$ at $x = L$ to determine the hydraulic head along the flow direction:

$$H(x) = \frac{\mu u}{\rho g k_o}\left[(L - x) + 2\delta\gamma_2\sigma_o(e^{-x/\delta} - e^{-L/\delta}) + \frac{\delta\gamma_2^2\sigma_o^2}{2}(e^{-2x/\delta} - e^{-2L/\delta})\right] \tag{24}$$

The normalized head loss across the entire filter is calculated by evaluating eq 24 at $x = 0$, dividing by $\Delta H_o = (\mu u L)/(\rho g k_o)$, and substituting eq 22 for σ_o to give

$$\frac{\Delta H}{\Delta H_o} = 1 + 2\gamma_2\sigma + \frac{\gamma_2^2\sigma^2 L}{2\delta}\frac{(1 - e^{-2L/\delta})}{(1 - e^{-L/\delta})^2} \tag{25}$$

which reduces to eq 10 in the limit of large δ. Similar equations may be evaluated over intermediate filter lengths. It is possible to adjust (γ_2, δ) to minimize the deviation between expressions similar to eq 25 and the corresponding data from the entire filter, top segment and bottom segment (Supporting Information, Table S1). Note that the normalized permeability, k/k_o, is the reciprocal of $\Delta H/\Delta H_o$ evaluated over the corresponding filter segment.

Three of the four data sets with intermediate head loss data were successfully described by fitting this two-parameter model to head loss data for the top and bottom segments and specific deposit data averaged over the entire filter. An example from Veerapaneni (*23*) is given in Figure 6. Additional examples from Chang (*19*) and Al-Abduwani (*24*) are given in Supporting Information, Figures S21 and S22, respectively. Data from Perera (*18*) were poorly described by this model, consistent with the results from the filter-averaged model.

The two-parameter model can be tested for Chang (*19*) and Al-Abduwani (*24*) by comparing the particle penetration depth, δ, fitted to head loss data to the δ determined by analysis of the deposit distribution, $\sigma(x)$, which was not used for model fitting. With data from Chang (*19*), the model overestimates particle penetration depth, δ, by a factor of 2 (Supporting Information, Table S2). This suggests that deposits are more concentrated near the inlet than expected for exponential $\sigma(x)$ and constant γ_2. Assuming $\sigma(x)$ is

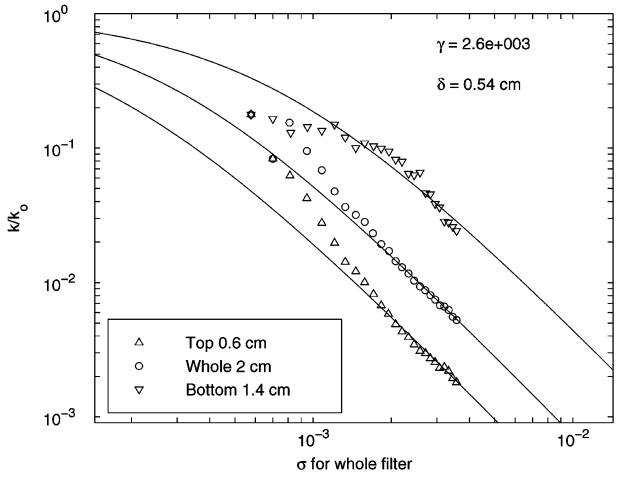

FIGURE 6. Permeability in the top 0.6 cm, whole 2 cm, and bottom 1.4 cm versus filter-averaged specific deposit for the experiment by Veerapaneni (*23*), where $u = 0.070$ cm/s. Curves are the fitted depth-dependent clogging model.

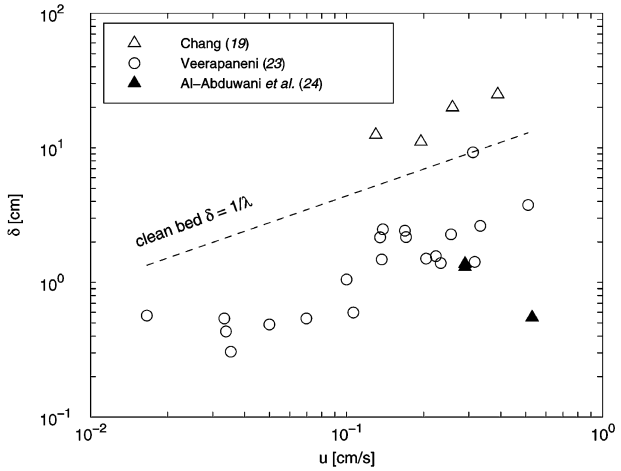

FIGURE 7. Depth-dependent model parameter δ versus velocity, u. The dashed line is the predicted $\delta = 1/\lambda$, where λ is the clean bed filtration coefficient for particles the same size as Veerapaneni's (*23*).

exponential, as indicated by Figure 5, this overestimate of δ suggests that the morphology parameter γ_2 is not constant but increases with depth in the column due to deposit compaction near the inlet, where the head gradient is largest, resulting in deposits with less effective surface area. This possibility is consistent with the known rearrangement of aggregates in shear flow (*34*) and deposit reconfiguration within filters (*15*, *26*). In contrast, the model significantly underestimates δ for data from Al-Abduwani et al. (*24*), shown in Supporting Information, Table S2. This may result from the uncertainty imposed by measuring head loss over the top 30-mm section of the column.

Fitted values of the characteristic distance of particle penetration, δ (Figure 7), and the morphology parameter, γ_2 (Figure 8) versus velocity indicate power law relationships for Chang (*19*) and Veerapaneni (*23*). Results from Al-Abduwani et al. (*24*) are uncertain due to their reported variability in flow rate, but estimated error bars have not been calculated for the depth-dependent model. The penetration parameter δ increases with fluid velocity. For comparison, Figure 7 also shows the reciprocal of the clean bed filtration coefficient, λ, which is a characteristic depth of penetration for a clean filter (*2*). The calculated λ^{-1} assumes particles the same size as Veerapaneni's (*23*), and the values

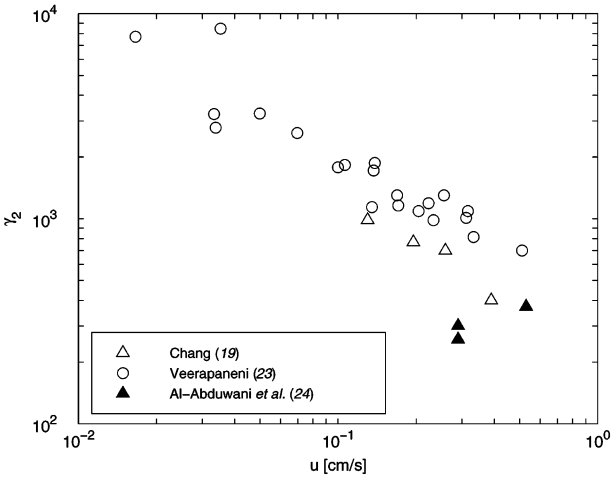

FIGURE 8. Depth-dependent model parameter γ_2 versus velocity.

are ~1 order of magnitude greater than the fitted values of δ, consistent with reduced particle penetration due to filter ripening.

The two-parameter model fitting arrived at values of γ_2 that are similar to γ from the one-parameter model (~15% less, with similar velocity dependence), so accounting for the depth of particle penetration did not significantly change the morphology parameter. The limited data available indicate that deposit morphology is the controlling influence, as suggested by Wiesner and others (*12*, *15*, *32*), rather than depth dependence, as argued by Lawler and others (*10*).

Discussion

Interpretation of O'Melia and Ali Model. Particle deposition and deposit morphology depend on the characteristics of the porous media, the depositing particles and the fluid flow field. A dimensionless number that represents these independent parameters for small particles is the Peclet number, which is the ratio of advective transport of particles to their Brownian transport near a collector surface. The Peclet number is

$$Pe = ud_c/D_p \tag{26}$$

where D_p is the particle diffusivity, given by

$$D_p = \kappa T/3\pi\mu d_p \tag{27}$$

where $\kappa = 1.38 \times 10^{-16}$ g cm^2 K^{-1} s^{-2} is Boltzmann's constant and T is the absolute temperature.

The empirically determined values of γ from all data sources are plotted in Figure 9 as a function of the Peclet number. The data from Narayan et al. (*11*), Tobiason and Vigneswaran (*21*), Veerapaneni (*23*), and Al-Abduwani et al. (*24*) were for experiments that used nearly spherical particles of known size. In normalizing the other two data sets, the primary particle size was estimated as 1 μm for the kaolinite used by Chang (*19*) and as 0.1 μm for the iron hydroxide particles within the flocs used by Boller and Kavanaugh (*22*). The correlation in Figure 9 appears as

$$\gamma = (1.0 \times 10^6)Pe^{-0.55} \tag{28}$$

This generalization of available filtration data is remarkable given the 10^2 range in fluid velocities, the 10^2 range in particle size, and the 10^1 range in collector size.

The observed power law correlation between γ and Peclet number reflects the tradeoff between advective and diffusive transport of particles up to and within a particle deposit. At small values of the Peclet number, diffusive transport

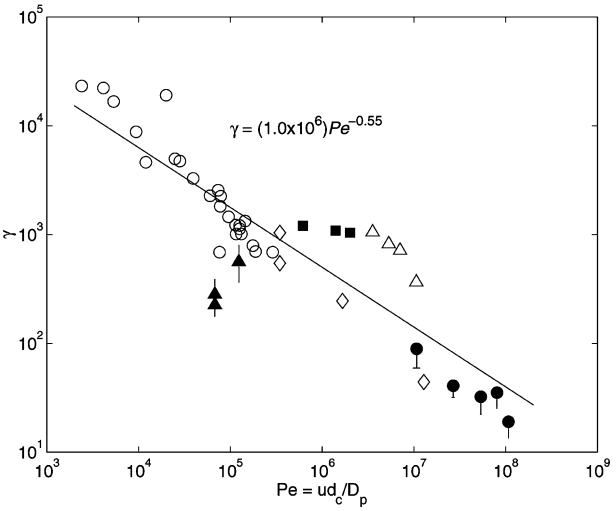

FIGURE 9. Fitted O'Melia and Ali parameter γ versus Peclet number: ● Narayan et al. (*11*); △ Chang (*19*); ◇ Tobiason and Vigneswaran (*21*); ■ Boller and Kavanaugh (*22*); ○ Veerapaneni (*23*); ▲ Al-Abduwani et al. (*24*). The solid line is the linear regression of ln(γ) versus ln(*Pe*). Estimated error bars for γ are plotted only for Narayan et al. (*11*) and Al-Abduwani et al. (*24*).

dominates over advective transport and this leads to porous, open deposits where flow resistance per deposited particle is large causing high values of γ. At larger values of the Peclet number, advective transport dominates over diffusive and this forms ballistic deposits that are more compact and have low flow resistance per deposited particle causing smaller values of γ. This agrees with the conceptual framework proposed by Veerapaneni and Wiesner (*12*, *15*, *32*), who argued that the fractal dimension of the deposit, which depends on the Peclet number, is a fundamental variable in clogging processes.

Interpretation of Cake Filtration Model. The cake model provides an alternative way to model clogging. To our knowledge, this is the first time a constitutive equation from cake models has been employed to model the evolution of deposit permeability as filtration proceeds. Physically, the parameter Θ is the head loss above which cake compression begins, representing the strength of the deposit (*31*). This suggests that the increased head loss observed at slower flow velocities results from the formation of weak deposits, whose permeability declines more for a given head loss across the deposit. This notion of deposit strength is in contrast to the conceptual understanding in the deep-bed filtration model, which assumes that fluid velocity determines the deposit's specific area.

The cake model has both advantages and disadvantages compared to the O'Melia and Ali model. The cake model explicitly accounts for deposit evolution, a real physical process, by modeling the feedback between deposit permeability and head loss across the deposit. At least in the case of Veerapaneni (*23*), the cake model demonstrates consistent correlation of the model parameter Θ with velocity, which substantiates the importance of fluid velocity in determining the permeability of clogging systems. However, since it contains two adjustable parameters, the cake model is susceptible to overfitting. Furthermore, because there is no physical basis for the constitutive relationship between head loss and cake permeability, the two adjustable parameters appear in what is essentially an adjustable equation. On the whole, the cake model may be preferable in situations where deposit evolution is important, since deposit evolution is not included in the deep-bed filtration model. In the context of this paper, it also highlights the important point that empirical models based on bulk-averaged filtration data are not unique.

Implications. Previous researchers have recognized the importance of deposit morphology during long-term particle retention in saturated porous media (*1*, *12*, *15*, *22*, *29*, *32*, *35*). We demonstrate there is a consistent relationship between head loss data and imposed flow velocity using either a modified O'Melia and Ali model or a cake filtration model. Detailed analysis of the O'Melia and Ali model suggests its parameter γ represents deposit morphology and is correlated to the collector Peclet number in six of eight data sets, as shown in Figure 9. Since particle clogging is important in engineered and natural systems, there is now a means to quantitatively relate permeability reduction to water velocity and particle accumulation.

A number of very significant issues remain. First, available experimental results have not demonstrated a steady-state condition, where there is no net accumulation of particles and the head loss is constant. Second, most laboratory experiments are conducted under constant-flow conditions while many situations operate under constant-head conditions, which would suggest that deposit morphology changes with time as the velocity decreases. Finally, as noninvasive pore level measurement of deposit configuration becomes available, a more mechanistic understanding of clogging may be possible.

Nomenclature

A_c	surface area per collector (L^2)
A_p	surface area per particle (L^2)
b	defined by eq 19 (T)
d_c	collector diameter (L)
d_p	particle diameter (L)
D_p	particle diffusivity ($L^2\ T^{-1}$)
g	acceleration of gravity ($L\ T^{-2}$)
ΔH	head loss (L)
ΔH_c	head loss across cake (L)
ΔH_o	clean bed head loss (L)
k	permeability (L^2)
k_c	cake permeability (L^2)
$k_{c,o}$	uncompressed cake permeability (L^2)
k_o	clean bed permeability (L^2)
L	filter depth (L)
L_c	cake thickness (L)
M	specific area (L^{-1})
M_o	clean bed specific area (L^{-1})
N	number of particles per collector (−)
Pe	Peclet number (−)
t	time (T)
T	absolute temperature (θ)
u	approach velocity ($L\ T^{-1}$)
V_c	volume per collector (L^3)
V_p	volume per particle (L^3)
x	distance (L)

Greek Letters

β'	specific area parameter (−)
γ	clogging parameter (−)

γ_2	morphology parameter in two-parameter model (−)
δ	penetration depth parameter in two-parameter model (L)
ϵ	porosity (−)
ϵ_c	cake porosity (−)
κ	Boltzmann's constant (M L^2 θ^{-1} T^{-2})
μ	dynamic viscosity (M L^{-1} T^{-1})
ρ	density (M L^{-3})
σ	specific deposit (−)
σ_o	specific deposit at $x = 0$ (−)
σ^*	normalized specific deposit defined in eq 20 (−)
Θ	cake compression parameter (L)

Acknowledgments

This research was supported by the Office of Civilian Radioactive Waste Management Fellowship (to D.C.M.), administered by Oak Ridge Institute for Science and Education under a contract between the U.S. Department of Energy and Oak Ridge Associated Universities, and by the NIEHS Superfund Basic Research Program, Grant 3PH2 ES04705. Data from the literature were digitized with the freeware program DataThief. The authors thank Aaron Packman and two anonymous reviewers for their suggestions, and especially Srinivas Veerapaneni and Mark Wiesner for their assistance in accessing Veerapaneni's (*23*) data.

Supporting Information Available

Tables showing fitted parameter values for the three models and 43 experiments; figures, taken with those in the main text, showing all the data analyzed. This material is available free of charge via the Internet at http://pubs.acs.org.

Literature Cited

(1) Tien, C. *Granular Filtration of Aerosols and Hydrosols*; Butterworth: Boston, 1989.

(2) McDowell-Boyer, L. M.; Hunt, J. R.; Sitar, N. Particle transport through porous media. *Water Resour. Res.* **1986**, *22*(13), 1901−1921.

(3) Ryan, J. N.; Elimelech, M. Colloid mobilization and transport in groundwater. *Colloids Surf., A* **1996**, *107*, 1−56.

(4) Kretzschmar, R.; Borkovec, M.; Grolimund, D.; Elimelech, M. Mobile subsurface colloids and their role in contaminant transport. *Adv. Agron.* **1999**, *66*, 121−193.

(5) Baveye, P.; Vandevivere, P.; Hoyle, B. L.; DeLeo, P. C.; Sanchez de Lozada, D. Environmental impact and mechanisms of the biological clogging of saturated soils and aquifer materials. *Crit. Rev. Environ. Sci. Technol.* **1998**, *28* (2), 123−191.

(6) Packman, A. I.; MacKay, J. S. Interplay of stream-surface exchange, clay particle deposition, and streambed evolution. *Water Resour. Res.* **2003**, *39* (4), 1097.

(7) Brodsky, E. E.; Roeloffs, E.; Woodcock, D.; Gall, I.; Manga, M. A mechanism for sustained groundwater pressure changes induced by distant earthquakes. *J. Geophys. Res.* **2003**, *108* (B8), 2390.

(8) Quirk, J. P.; Schofield, R. K. The effect of electrolyte concentration on soil permeability. *J. Soil Sci.* **1955**, *6* (2), 163−178.

(9) Kia, S. F.; Fogler, H. S.; Reed, M. G. Effect of pH on colloidally induced fines migration. *J. Colloid Interface Sci.* **1987**, *118* (1), 158−168.

(10) Kau, S. M.; Lawler, D. F. Dynamics of deep-bed filtration: velocity, depth and media. *J. Environ. Eng.* **1995**, *121* (12), 850−859.

(11) Narayan, R.; Coury, J. R.; Masliyah, J. H.; Gray, M. R. Particle capture and plugging in packed-bed reactors. *Ind. Eng. Chem. Res.* **1997**, *36* (11), 4620−4627.

(12) Veerapaneni, S.; Wiesner, M. R. Deposit morphology and head loss development in porous media. *Environ. Sci. Technol.* **1997**, *31* (10), 2738−2744.

(13) Cleasby, J. L.; Williamson, M. M.; Baumann, E. R. Effect of filtration rate changes on quality. *J. Am. Water Works Assoc.* **1963**, *55*, 869−877.

(14) Bai, R.; Tien, C. Particle detachment in deep bed filtration. *J. Colloid Interface Sci.* **1997**, *186*, 307−317.

(15) Wiesner, M. R. Morphology of particle deposits. *J. Environ. Eng.* **1999**, *125* (12), 1124−1132.

(16) Burganos, V. N.; Skouras, E. D.; Parakeva, C. A.; Payatakes, A. C. Simulation of the dynamics of depth filtration of non-Brownian particles *AIChE J.* **2001**, *47* (4), 880−894.

(17) Lee, J.; Koplik, J. Network model for deep bed filtration. *Phys. Fluids* **2001**, *13* (5), 1076−1078.

(18) Perera, Y. A. P. Comparison of performance of radial and upflow filters. M.S. Thesis EV-82-10, Asian Institute of Technology, Bangkok, Thailand, 1982.

(19) Chang, J. W. Mathematical modeling of deep bed filtration: microscopic approach. M.S. Thesis EV-85-3, Asian Institute of Technology, Bangkok, Thailand, 1985.

(20) Vigneswaran, S.; Chang, J. S. Experimental testing of mathematical models describing the entire cycle of filtration. *Water Res.* **1989**, *23* (11), 1413−1421.

(21) Tobiason, J. E.; Vigneswaran, B. Evaluation of a modified model for deep bed filtration. *Water Res.* **1994**, *28* (2), 335−342.

(22) Boller, M. A.; Kavanaugh, M. C. Particle characteristics and headloss increase in granular media filtration. *Water Res.* **1995**, *29* (4), 1139−1149.

(23) Veerapaneni, S. Formation and morphology of colloidal deposits in porous media. Ph.D. Thesis, Rice University, Houston, TX, 1996.

(24) Al-Abduwani, F. A. H.; Shirzadi, A.; van den Broek, W. M. G. T.; Currie, P. K. Formation damage vs solid particles deposition profile during laboratory simulated PWRI. SPE-82235. European Formation Damage Conference, The Hague, The Netherlands, 13−14 May 2003.

(25) Wright, A. M. Filtration modelling. Ph.D. Thesis, University of California, Berkeley, 1982.

(26) Hunt, J. R.; Hwang, B.-C.; McDowell-Boyer, L. M. Solids accumulation during deep bed filtration. *Environ. Sci. Technol.* **1993**, *27* (6), 1099−1107.

(27) O'Melia, C. R.; Ali, W. The role of retained particles in deep bed filtration. *Prog. Water Res.* **1978**, *10* (5/6), 167−182.

(28) Bear, J. *Dynamics of Fluids in Porous Media*; Dover: New York, 1972.

(29) Darby, J. L.; Attanasio, R. E.; Lawler, D. F. Filtration of heterodisperse suspensions: Modeling of particle removal and head loss. *Water Res.* **1992**, *26* (6), 711−726.

(30) Tiab, D.; Donaldson, E. *Petrophysics*; Gulf Publishing Co.: Houston, TX, 1996.

(31) Lee, D. J.; Wang, C. H. Theories of cake filtration and consolidation and implications to sludge dewatering. *Water Res.* **2000**, *34* (1), 1−20.

(32) Veerapaneni, S.; Wiesner, M. R. Particle deposition on an infinitely permeable surface. *J. Colloid Interface Sci.* **1994**, *162* (1), 110−122.

(33) Bedrikovetsky, P.; Marchesin, D.; Shecaira, F.; Souza, A. L.; Milanez, P. V.; Rezende, E. Characterization of deep bed filtration system from laboratory pressure drop experiments. *J. Petrol. Sci. Eng.* **2001**, *32* (2−4), 167−177.

(34) Sonntag, R. C.; Russel, W. B. Structure and breakup of flocs subjected to fluid stresses. *J. Colloid Interface Sci.* **1986**, *113* (2), 399−413.

(35) Elimelech, E.; Gregory, J.; Jia, X.; Williams, R. A. *Particle Deposition and Aggregation*; Butterworth-Heinemann: Oxford, U.K., 1995.

Received for review April 26, 2004. Revised manuscript received October 8, 2004. Accepted October 18, 2004.

ES049367K